Aust. J. Phys., 1992, **45**, 651–69

Ab Initio Ro–Vibrational Structure of the $C_{2\nu}$ Isotopes of H_2O^+

*F. Wang and E. I. von Nagy-Felsobuki**

Department of Chemistry, University of Newcastle,
Callaghan, N.S.W. 2308, Australia.
* Author to whom correspondence should be addressed.

Abstract

The ro–vibrational structures of the $C_{2\nu}$ isotopes of H_2O^+ have been calculated from variational solution of the normal coordinate Eckart–Watson Hamiltonian. The calculations use the discrete ab initio potential energy surface of Weis *et al.* (1989). Where comparisons can be made, the assignment of the vibrational states is in excellent agreement with experiment and with the ab initio variational calculation of Weis *et al.*, who utilised a different force field and an internal coordinate nuclear Hamiltonian (instead of the Eckart–Watson Hamiltonian). Furthermore, the calculated rotational levels of the ground and the first excited vibrational states of H_2O^+ and D_2O^+ are in excellent agreement with experiment.

1. Introduction

Attempts to solve the 'complete' molecular Schrödinger equation are not commonplace, even with the advent of supercomputers. Searles and von Nagy-Felsobuki (1991*a*) have previously defined the 'complete' problem as from calculating a Born–Oppenheimer potential energy (PE) surface to variationally solving the ro–vibrational Hamiltonian. Perhaps the most celebrated example in the modern literature is H_3^+. With two electrons and three protons it is the simplest triatomic molecule in chemistry. Quantal investigations by Carney and Porter (1976, 1980) of its infrared spectrum near the potential energy minimum have predicted and substantiated experimental observations.

Even for simple triatomic systems, ro–vibrational Hamiltonians are found to be problematic. As Sutcliffe (1990) has shown, Eckhart's notion of an embedded equilibrium geometry for a stable triatomic molecule necessarily leads to different ro–vibrational Hamiltonians for bent and linear nuclear configurations (as derived by Watson 1968, 1970). Simply put, for a bent triatomic molecule with $3N-6$ degrees of freedom, singularities in the mass-dependent potential energy operator cannot yield a smooth transition to a linear triatomic molecule with $3N-5$ degrees of freedom. This led Tennyson and Sutcliffe (1984) to develop a ro–vibrational Hamiltonian in terms of a body-fixed scattering coordinate system in which the triatomic molecule (denoted as ABC) is considered in terms of the interaction of a diatomic component (AC) with a scattering atom (B). Hence, the embedded equilibrium structure has been circumvented by introducing a non-rigid system. The success of this ro–vibrational Hamiltonian in interpreting and predicting the ro–vibrational states of H_3^+ has been well documented by Miller *et al.* (1989).

0004-9506/92/050651$05.00

Recently, Searles and von Nagy-Felsobuki (1991*b*) developed the most general form of the Eckart–Watson Hamiltonian, which is applicable to a triatomic system. The ro–vibrational Hamiltonian is based on rectilinear displacement coordinates, but is applicable to the C_S case and so collapses to the Carney and Porter (1976) D_{3h} and the Carney *et al.* (1977) C_{2v} Hamiltonians. Moreover, Hendersen *et al.* (1988) and Searles and von Nagy-Felsobuki (1989) demonstrated that for Li_3^+ the scattering coordinate solution yields essentially the same vibrational band origins as the normal coordinate solution. These vastly different solution algorithms (but which employed the same electronic force field) gave the same assignment and moreover, yielded the first ten vibrational band origins of $^7Li_3^+$ and $^6Li^7Li_2^+$ to within $0{\cdot}03\ cm^{-1}$, therefore indicating that both algorithmic approaches have properly converged in describing small amplitudes of vibration.

As has been pointed out by Herzberg (1980), perhaps one of the most important triatomic ions is H_2O^+, which is found in a variety of environments such as the earth's atmosphere, interstellar space and oxygen-rich circumstellar envelopes. Lew (1976), Strahan *et al.* (1986) and Dinelli *et al.* (1988) have reported high resolution spectra for the vibrational ground state, the ν_1, $2\nu_2$ and $3\nu_2$ and ν_3 vibrational states for the electronic ground state (χ^2B_1) of this ion. For D_2O^+, Lew and Groleau (1987) have reported data on the vibrational ground state and the ν_2 and $3\nu_3$ vibrational states. Karlsson *et al.* (1975), using photoelectron spectroscopy, have provided data on the higher overtones of H_2O^+, D_2O^+ and HDO^+. However, there is little information on the other C_{2v} isotopes of this molecule, which although not abundant, nevertheless would be of interest with respect to interstellar searches.

More pertinent to this study is the work of Weis *et al.* (1989), who have theoretically resolved the infrared spectrum of H_2O^+, D_2O^+ and HDO^+ using the 'complete' approach. That is, they have calculated a multiconfiguration reference configuration interaction (MRCI) discrete potential energy surface and embedded an analytical representation of it in an internal coordinate ro–vibrational Hamiltonian, which they have variationally solved using basis functions constructed from Morse, harmonic oscillator and associate Legendre functions.

As an extension of our earlier work (see Searles and von Nagy-Felsobuki 1991*a*, 1991*b*), we report here the ab initio ro–vibrational structure of the C_{2v} isotopes of H_2O^+. Although we have employed the discrete MRCI potential of Weis *et al.* (1989), we have utilised a different force field embedded within the Eckart–Watson Hamiltonian and have used different ro–vibrational trial functions in our variational solution. Nevertheless, we will show that our t coordinate solution produces ro–vibrational eigenenergies in excellent agreement with the internal coordinate solution of Weis *et al.* (1989) and with experiment for the isotopes (where comparison can be made). Furthermore, we report theoretically determined ro–vibrational states for the C_{2v} isotopes, where no experimental or ab initio data are currently available.

2. Analytical Representation of the PE Surface

Weis *et al.* (1989) have calculated an extensive discrete PE surface of the ground electronic state of H_2O^+ using highly correlated MRCI electronic wavefunctions. Their analytical representation of the 50 point surface involved fitting a polynomial expansion in Simon–Parr–Finlan bond stretching coordinates and a cubic expansion

in terms of an angle bending coordinate. All calculated MRCI electronic energies were reproduced with a root-mean-square error of $\sim 3\times10^{-6}E_h$. However, as Burton *et al.* (1985) have emphasised, the root-mean-square error is only one criterion with respect to the suitability of an analytical representation. For example, it is important that the analytical representation is consistent with anticipated physical properties and is smooth with no singularities in the potential energy integration region. Within the guidelines set by Burton *et al.* (1985) it is unclear which is the optimum form of the expansion variable in a power series expansion involving the angle bending coordinate (such as the one used by Weis *et al.* 1989). Hence, when dealing with bent triatomic systems, Burton *et al.* (1985), Searles *et al.* (1988) and Searles and von Nagy-Felsobuki (1991*b*, 1991*c*) have used power series expansions involving expansion variables which are a function of the instantaneous bond length R_i. Such expansions are particularly useful in constructing effective configuration interaction trial wavefunctions for the three-dimensional solution of the nuclear Schrödinger equation.

Following Searles and von Nagy-Felsobuki (1991*b*, 1991*c*) we have refitted the discrete surface of Weis *et al.* (1989) using Padé approximates. The Padé approximates are rational functions in which the numerator and denominator are power series expansions (of order m and n respectively) of the expansion variables ρ_i:

$$P(m,n) = \sum_{i=0}^{m}\sum_{j=0}^{m}\sum_{k=0}^{m} a_{ijk}\,\rho_1^i\,\rho_2^i\,\rho_3^k \Big/ \sum_{i'=0}^{n}\sum_{j'=0}^{n}\sum_{k'=0}^{n} b_{i'j'k'}\,\rho_1^{i'}\,\rho_2^{j'}\,\rho_3^{k'}\,, \qquad (1)$$

such that $(i+j+k) \le m$ and $(1'+j'+k') \le n$ and where

$$\rho_i = 2(R_i - R_e)/(R_i + R_e)\,. \qquad (2)$$

Here R_i and R_e are the instantaneous and equilibrium bond lengths respectively. The Ogilvie (1981) expansion variable (given by equation 2) has a well defined quantum mechanical basis.

The coefficients of the fit are given in Table 1 and were obtained using the singular value decomposition (SVD) analysis. SVD enables identification of terms in the power series expansions which have a marked effect on the magnitude of the coefficients, but an insignificant effect on the root-mean-square. Hence, if these expansion variables are excluded (i.e. by zeroing the singular values denoted by σ), the fit will not be significantly degraded (see Burton *et al.* 1985). Table 1 shows that the root-mean-square error of the fit is $2\cdot6\times10^{-5}E_h$. Numerous graphical inspections of the surface were performed in order to ensure that no oscillatory behaviour or singularities were present in the potential energy integration region. For example, we were able to obtain a $P(3,6)$ surface with a root-mean-square error of $6\cdot3\times10^{-6}$ E_h provided that singular values σ_{49}, σ_{51}–σ_{60} were zeroed. However, on graphical inspection the surface was found to have singularities present in the t_2–t_3 integration region. Hence, such a surface is not suitable for embedding in the nuclear Schrödinger equation. However, by zeroing an additional singular value σ_{45}, an artifact free surface was obtained, even though the root-mean-square error of the fit is one magnitude larger. Fig. 1

Table 1. Expansion coefficients for the $P(3,6)$ power series representation of the PE surfaces of H_2O^+

Units of all coefficients are in a.u. A full description of Padé approximates and notation used is given by Searles and von Nagy-Felsobuki (1991*c*). The singular values σ_{45}, σ_{49}, σ_{51}–σ_{60} were zeroed in order to ensure no oscillatory behaviour or singularities in the integration region

	Expansion variable	Numerator	Denominator		Expansion variable	Numerator	Denominator
1	1	−75·88840	1·00000	27	$\rho_1\rho_3^4+\rho_2\rho_3^4$	0·00000	0·10051
2	$\rho_1+\rho_2$	−0·00289	0·00009	28	$\rho_1^3\rho_2^2+\rho_1^2\rho_2^3$	0·00000	−0·01335
3	ρ_2^3	0·00758	0·00003	29	$\rho_1^3\rho_3^2+\rho_2^3\rho_3^2$	0·00000	−0·02313
4	$\rho_1^2+\rho_2^2$	0·00167	−0·01123	30	$\rho_1^2\rho_3^3+\rho_2^2\rho_3^3$	0·00000	−0·03330
5	ρ_3^2	0·00281	−0·00745	31	$\rho_1^3\rho_2\rho_3+\rho_1\rho_2^3\rho_3$	0·00000	0·03192
6	$\rho_1\rho_2$	0·00148	−0·00254	32	$\rho_1\rho_2\rho_3^3$	0·00000	−0·15018
7	$\rho_2\rho_3+\rho_1\rho_3$	−0·00070	0·00619	33	$\rho_1^2\rho_2^2\rho_3$	0·00000	0·02214
8	$\rho_1^3+\rho_2^3$	−0·00032	0·01424	34	$\rho_1^2\rho_2\rho_3^2+\rho_1\rho_2^2\rho_3^2$	0·00000	0·02854
9	ρ_3^3	0·00149	−0·01355	35	$\rho_1^6+\rho_2^6$	0·00000	0·00040
10	$\rho_1^2\rho_2+\rho_2^2\rho_1$	−0·00090	0·00695	36	ρ_3^6	0·00000	−0·11660
11	$\rho_1^2\rho_3+\rho_2^2\rho_3$	0·00071	−0·01012	37	$\rho_1^5\rho_2+\rho_2^5\rho_1$	0·00000	−0·00020
12	$\rho_1\rho_3^2+\rho_2\rho_3^2$	−0·00014	0·02324	38	$\rho_1^5\rho_3+\rho_2^5\rho_3$	0·00000	−0·01429
13	$\rho_1\rho_2\rho_3$	0·00085	−0·02884	39	$\rho_1\rho_3^5+\rho_2\rho_3^5$	0·00000	0·19406
14	$\rho_1^4+\rho_2^4$	0·00000	−0·00909	40	$\rho_1^4\rho_2^2+\rho_2^4\rho_1^2$	0·00000	−0·05428
15	ρ_3^4	0·00000	−0·02489	41	$\rho_1^4\rho_3^2+\rho_2^4\rho_3^2$	0·00000	0·03911
16	$\rho_1^3\rho_2+\rho_2^3\rho_1$	0·00000	−0·00498	42	$\rho_1^2\rho_3^4+\rho_2^2\rho_3^4$	0·00000	−0·09080
17	$\rho_1^3\rho_3+\rho_2^3\rho_3$	0·00000	0·00587	43	$\rho_1^4\rho_2\rho_3+\rho_2^4\rho_1\rho_3$	0·00000	0·04773
18	$\rho_1\rho_3^3+\rho_2\rho_3^3$	0·00000	0·04830	44	$\rho_1\rho_2\rho_3^4$	0·00000	−0·44941
19	$\rho_1^2\rho_2^2$	0·00000	−0·01122	45	$\rho_1^3\rho_2^3$	0·00000	−0·08927
20	$\rho_1^2\rho_3^2+\rho_2^2\rho_3^2$	0·00000	−0·02896	46	$\rho_1^3\rho_3^3+\rho_2^3\rho_3^3$	0·00000	−0·03002
21	$\rho_1^2\rho_2\rho_3+\rho_1\rho_2^2\rho_3$	0·00000	0·03843	47	$\rho_1^3\rho_2^2\rho_3+\rho_1^2\rho_2^3\rho_3$	0·00000	0·33846
22	$\rho_1\rho_2\rho_3^2$	0·00000	−0·07975	48	$\rho_1^3\rho_2\rho_3^2+\rho_1\rho_2^3\rho_3^2$	0·00000	−0·20638
23	$\rho_1^5+\rho_2^5$	0·00000	0·00118	49	$\rho_1^2\rho_2\rho_3^3+\rho_1\rho_2^2\rho_3^3$	0·00000	0·41913
24	ρ_3^5	0·00000	−0·06241	50	$\rho_1^2\rho_2^2\rho_3^2$	0·00000	−0·64414
25	$\rho_1^4\rho_2+\rho_2^4\rho_1$	0·00000	−0·01075				
26	$\rho_1^4\rho_3+\rho_2^4\rho_3$	0·00000	0·01741				
					$(\chi^2)^{1/2}/E_h$	2·6 by 10^{-5}	

gives the energy contour plots of the $P(3,6)$ surface, given in Table 1, in terms of the rectilinear t coordinates. No singularities are present in this and in numerous other two-dimensional cuts of the surface.

3. Ro–Vibrational Hamiltonian and Solution Algorithm

The vibrational Hamiltonian used in this study is the t coordinate Hamiltonian derived by Carney *et al.* (1977), which differs significantly from the internal coordinate Hamiltonian used by Weis *et al.* (1989). The rectilinear Hamiltonian has the form

$$\hat{H} = \hat{T}_v + \hat{T}_l + \hat{U}_w + \hat{V}$$

$$= -\frac{\hbar^2}{2M_r}\sum_{i=1}^{3}\frac{\partial^2}{\partial t_i^2} - \frac{\hbar^2}{2I'_{zz}(t_1)}\left(t_3\frac{\partial}{\partial t_2} - t_2\frac{\partial}{\partial t_3}\right)^2 - \frac{\hbar^2}{8}\sum_{\alpha}\mu_{\alpha\alpha} + \hat{V}, \qquad (3)$$

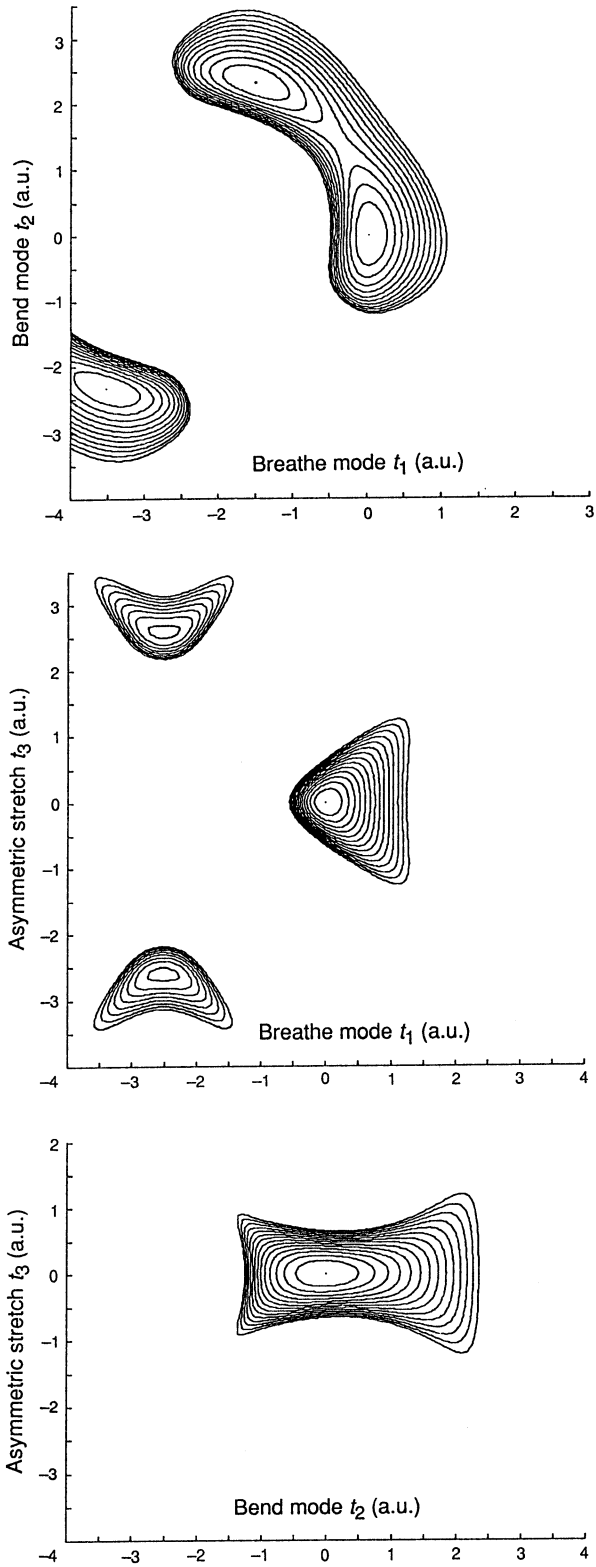

Fig. 1. Two-dimensional constant potential energy plots for the $P(3,6)$ surface with SVD analysis and with singular values σ_{45}, σ_{49} and σ_{51}–σ_{60} zeroed.

where the first term is the vibrational kinetic energy contribution, the second term is the vibrational angular momentum contribution and the third is the Watson term, which is a mass-dependent contribution to the potential energy operator.

The Watson operator is the sum of the diagonal elements of the reciprocal effective moment of the inertial tensor. A perturbation expression for this operator can be derived and is valid for small amplitudes of vibration. Hence, as shown by Searles and von Nagy-Felsobuki (1991*b*), it can be incorporated in the vibrational Hamiltonian, thereby avoiding the embedded singularities.

The basic approach to the variational solution of equation (3) used in this work has been detailed by Doherty *et al.* (1986). If differs vastly from the variational approach used by Weis *et al.* (1989), who constructed their three-dimensional basis functions from Morse (asymmetric stretch functions), harmonic oscillator (breathe functions) and associate Legendre functions (angle bending functions), and who used analytical/numerical techniques to evaluate the necessary integrals. In order to emphasise the differences in the two solution algorithms, the following points need to be made about our approach. The one-dimensional wavefunctions are calculated using a finite-element solution of a one-dimensional Hamiltonian, which is expressed in terms of a single rectilinear t coordinate. In the one-dimensional Hamiltonian only the first-order expansion of the Watson operator was used, since it is diagonal in the t coordinates. For each t coordinate, 1000 finite elements were constructed within the following domains: $t_1\,[-1{\cdot}7, 3{\cdot}5]$, $t_2\,[-2{\cdot}5, 4{\cdot}5]$, $t_3\,[-2{\cdot}0, 2{\cdot}0]$. A three-dimensional configuration basis was spliced from 20×20×20 one-dimensional eigenfunctions. The configuration list was selected using a nodal cut-off criterion; all products containing more than 13 nodes were excluded and so a total of 560 basis functions were employed. For the three-dimensional Hamiltonian, the third-order expansion of the Watson operator was used. The potential energy integrals were evaluated using the Harris *et al.* (1965) scheme, whereas all other integrals were evaluated using a 16 point Gauss quadrature scheme. Finally, the secular determinant was constructed using equation (3) and diagonalised to yield vibrational wavefunctions and eigenenergies, both of which are required for the ro–vibrational problem. Table 2 gives the lowest-lying 20 vibrational band origins and assignments for all the $C_{2\nu}$ isotopes of H_2O^+ and, furthermore, Table 3 compares the experimental vibrational band origins of H_2O^+ and D_2O^+ with the variational perturbation calculations of Weis *et al.* (1989).

The ro–vibrational Hamiltonian in vibration matrix representation, as given by Carney *et al.* (1977), is

$$\hat{H}_{ij}^{\mathrm{RV}} = E_i\langle S\rangle_{ij} + 0{\cdot}5\langle A\rangle_{ij}\hat{\Pi}_x^2 + 0{\cdot}5\langle B\rangle\hat{\Pi}_y^2 + 0{\cdot}5\langle C\rangle_{ij}\hat{\Pi}_z^2$$

$$+ 0{\cdot}5\langle D\rangle_{ij}(\hat{\Pi}_x\,\hat{\Pi}_y + \hat{\Pi}_y\,\hat{\Pi}_x) + \mathrm{i}/\hbar\langle F\rangle_{ij}\hat{\Pi}_z\,, \qquad (4)$$

where E_i is the ith pure vibrational eigenenergy, $\langle S\rangle_{ij}$ is the overlap vibration matrix element and the $\hat{\Pi}$ are the rotational angular momentum operators,

Table 2. Zero-point energies (ZPE), vibrational band origins (in cm^{-1}) and assignment of the $C_{2\nu}$ isotopes of H_2O^+

$(\nu_1\,\nu_2\,\nu_3)^A$	$H_2{}^{16}O^+$	$D_2{}^{16}O^+$	$T_2{}^{16}O^+$	$H_2{}^{18}O^+$	$D_2{}^{18}O^+$	$T_2{}^{18}O^+$
ZPE	4096·5	3004·1	2536·5	4083·1	2995·0	2514·8
(010)	1412·1	1047·5	888·7	1406·3	1043·2	880·5
(020)	2780·7	2071·9	1760·9	2769·4	2063·4	1744·9
(100)	3212·5	2346·6	1968·6	3206·4	2345·0	1957·3
(001)	3255·0	2424·4	2067·2	3241·8	2412·9	2045·0
(030)	4098·5	3070·9	2615·3	4082·4	3058·5	2591·8
(110)	4611·4	3385·8	2851·2	4599·5	3379·8	2831·7
(011)	4641·5	3458·0	2945·9	4622·6	3442·2	2915·7
(040)	5353·9	4042·0	3450·8	5333·8	4026·0	3420·2
(120)	5970·8	4403·7	3718·4	5953·6	4393·6	3691·0
(021)	5988·1	4469·8	3808·9	5963·8	4449·9	3771·0
(200)	6300·0	4641·9	3904·4	6284·6	4637·4	3881·8
(101)	6312·2	4689·2	3978·9	6293·6	4676·1	3946·0
(002)	6476·4	4812·2	4103·1	6454·6	4791·4	4060·3
(050)	6529·5	4981·2	4265·7	6507·5	4962·1	4228·5
(130)	7278·1	5397·0	4568·1	7256·8	5383·1	4533·5
(031)	7288·0	5457·7	4654·9	7258·7	5433·9	4609·7
(060)	7631·2	5674·7	4782·9	7612·4	5665·2	4751·8
(210)	7681·3	5715·0	4851·9	7658·8	5697·4	4810·8
(111)	7686·8	5833·6	4972·1	7662·3	5808·7	4921·6

[A] Vibrational assignment is based on the weights of the coefficients (see text).

whose components are referred to the molecule-fixed coordinate system. The vibrationally averaged rotational constants are labelled $\langle A' \rangle_{ij}$, $\langle B' \rangle_{ij}$, $\langle C' \rangle_{ij}$ and $\langle D' \rangle_{ij}$. The matrix element $\langle F \rangle_{ij}$ is the Coriolis coupling term. The prime indicates the incorporation of the multiplying constant of $\frac{1}{2}$. Table 4 gives the vibrationally averaged rotational constant elements spanned by the lowest four vibrational states.

The full ro–vibrational wavefunction $\Psi(\boldsymbol{v}, \boldsymbol{r})$ is given by a linear combination of products of the vibrational wavefunctions $\Psi_n(\boldsymbol{v})$ (from the solution of equation 3) and symmetric-top rotor functions $\Phi_{jkm}(\boldsymbol{r})$:

$$\Psi(\boldsymbol{v}, \boldsymbol{r})_{jm} = \sum_{nk} C_{nkj}\, \Psi_n(\boldsymbol{v})\, \Phi_{jkm}(\boldsymbol{r})\,, \tag{5}$$

where the $\boldsymbol{v}$ and $\boldsymbol{r}$ denote the vibrational and rotational coordinates respectively.

In order to obtain a ro–vibrational Hamiltonian matrix representation containing real matrix elements, we used the plus and minus combinations of the regular symmetric-top eigenfunctions $R^{\pm}_{jkm}$ basis,

$$|R^{+}_{jkm}\rangle = \sqrt{\tfrac{1}{2}}\,\{|\Phi_{jkm}(\boldsymbol{r})\rangle + |\Phi_{j-km}(\boldsymbol{r})\rangle\}\,,$$

$$|R^{-}_{jkm}\rangle = \sqrt{\tfrac{1}{2}}\,\mathrm{i}\{|\Phi_{jkm}(\boldsymbol{r})\rangle - |\Phi_{j-km}(\boldsymbol{r})\rangle\}\,. \tag{6}$$

Table 3. Comparison of experimental with ab initio vibrational band origins (in cm^{-1}) of $H_2{}^{16}O^+$ and $D_2{}^{16}O^+$

	Experiment[A]	This work (variational solution	Weis *et al.* (1989) Variational solution	Weis *et al.* (1989) Perturbation solution
		(*a*) $H_2{}^{16}O^+$		
(010)	1408·4	1412·1	1410·4	1413·1
(020)	2771·3	2780·7	2774·2	2786·2
(100)	3213·0	3212·5	3211·0	3208·1
(001)	3259·0	3255·0	3255·0	3251·3
(030)	4085·0	4098·5	4083·6	4119·2
(110)	4593·0	4611·4	4600·1	4600·9
(011)	—	4641·5	4639·9	4637·9
(040)	—	5353·9	5323·4	5412·1
(120)	5936·0	5970·8	5942·3	5953·6
(021)	—	5988·1	5980·8	5984·5
(200)	6298·0	6300·0	6296·7	6282·2
(101)	—	6312·2	6310·2	6295·8
(002)	—	6476·4	6475·0	6466·2
(050)	—	6529·5	6462·9	6665·0
(130)	7234·0	7278·1	7228·6	7266·2
(031)	—	7288·0	7271·2	7291·0
(060)	7639·0	7631·2	7496·2	7650·9
(210)	—	7681·3	7662·2	7662·0
(111)	—	7686·8	7672·9	7830·1
		(*b*) $D_2{}^{16}O^+$		
(010)	1044·3	1047·5	1047·0	1048·1
(020)	2063·0	2071·9	2070·2	2074·5
(100)	2342·0	2346·6	2346·2	2345·2
(001)	—	2424·4	2424·2	2422·7
(030)	3058·7	3070·9	3067·5	3079·2
(110)	3373·0	3385·8	3382·2	3383·0
(011)	—	3458·0	3457·8	3457·0
(040)	—	4042·0	4035·8	4062·2
(120)	4396·0	4403·7	4393·6	4399·1
(021)	—	4469·8	4468·4	4469·6
(200)	4638·0	4641·9	4640·7	4636·0
(101)	—	4689·2	4688·5	4683·1
(002)	—	4812·2	4812·5	4807·5
(050)	—	4981·2	4970·5	5023·5
(130)	—	5397·0	5378·5	5393·5
(030)	—	5457·7	5454·4	5460·5
(060){210}[B]	5650·0	5674·7	5666·1	5662·9
(210){111}[B]	—	5715·0	5710·8	5707·1
(111){012}[B]	—	5833·6	5833·3	5828·5

[A] See Lew (1976), Lew and Groleau (1987), Strahan *et al.* (1986) and Reutt *et al.* (1986).
[B] Weis *et al.* (1989) assignment is given in curly brackets.

Carney *et al.* (1977) have detailed the matrix elements spanned by plus and minus combinations of the regular symmetric-top eigenfunctions, which incorporate the angular momentum operators. The H^{RV} matrix is constructed using the trial basis functions given by equations (5) and (6) and diagonalised yielding ro–vibrational eigenenergies and the ro–vibrational eigenfunctions. Table 5 gives the variationally

Table 4. Rotational constant and Coriolis matrix elements (in cm^{-1}) of C_{2v} isotopes of H_2O^+

ij	$H_2{}^{16}O^+$	$D_2{}^{16}O^+$	$T_2{}^{16}O^+$	$H_2{}^{18}O^+$	$D_2{}^{18}O^+$	$T_2{}^{18}O^+$
			(*a*) **A′**			
11	28·7944	15·8875	11·6751	28·4336	15·6206	11·3199
21	7·2378	3·2951	2·1800	−7·1343	3·2377	−2·1081
22	32·7619	17·3865	12·5701	32·3386	17·0936	12·1841
31	1·8454	0·7825	0·5121	−1·8012	0·7545	0·4819
32	12·1008	5·2580	3·4113	11·9195	5·1644	−3·2961
33	38·0600	19·2087	13·6189	37·5460	18·8833	13·1954
41	−2·8057	−1·4490	−1·0510	2·7412	1·3985	0·9934
42	0·5180	0·2274	0·1609	0·4848	−0·2062	0·1432
43	0·5827	0·2170	0·1358	0·5487	−0·2003	−0·1233
44	28·0332	15·6609	11·5773	27·6660	15·3831	11·2131
			(*b*) **B′**			
11	12·4109	6·2368	4·1938	2·4118	6·2808	4·1942
21	−1·2899	−0·5657	−0·3550	1·2845	−0·5662	0·3516
22	12·4455	6·2573	4·2083	12·4450	6·3004	4·2080
31	0·3807	0·1497	0·0895	−0·3756	0·1478	0·0872
32	−1·8146	−0·7983	−0·5008	−1·8073	−0·7992	0·4963
33	12·4383	6·2688	4·2187	12·4372	6·3113	4·2177
41	−1·2083	−0·4927	−0·2889	1·2148	0·5023	0·2932
42	−0·0295	−0·0397	−0·0379	−0·0199	0·0328	−0·0324
43	0·0037	0·0097	0·0092	0·0014	−0·0080	−0·0078
44	12·1563	6·1374	4·1339	12·1607	6·1829	4·1362
			(*c*) **C′**			
11	8·4622	4·4016	3·0422	8·4303	4·4021	3·0173
21	−0·0089	−0·0408	−0·0454	−0·0005	−0·0330	0·0388
22	8·5125	4·4157	3·0489	8·4815	4·4169	3·0242
31	0·1321	0·0598	0·0401	−0·1279	0·0572	0·0376
32	0·0190	−0·0487	−0·0595	0·0321	−0·0376	0·0502
33	8·5797	4·4328	3·0565	8·5500	4·4349	3·0322
41	−0·8381	−0·3691	−0·2305	0·8347	0·3700	0·2292
42	0·0092	−0·0043	−0·0076	0·0108	0·0025	−0·0057
43	0·0169	0·0067	0·0045	0·0161	−0·0062	−0·0040
44	8·2844	4·3356	3·0039	8·2533	4·3363	2·9797
			(*d*) **D′**			
11	0·1573−11	−0·1563−10	−0·1659−10	−0·6368−11	0·4447−11	0·1573−10
21	0·3445−12	0·2855−12	−0·5571−12	0·4989−12	0·4470−12	−0·5549−12
22	0·1535−11	−0·1629−10	−0·1696−10	−0·5876−11	0·4993−11	0·1563−10
31	0·1100−10	0·1360−12	−0·1497−11	0·5141−13	0·7720−13	−0·1100−11
32	0·4485−12	−0·1062−11	−0·6005−12	−0·1356−13	0·1327−12	−0·7510−12
33	0·2132−11	−0·1845−10	−0·1801−10	−0·6098−11	0·5456−11	0·1739−10
41	0·2214−10	−0·6691−10	−0·4251−10	0·5205−10	−0·3694−10	−0·3171−10
42	0·1343−10	−0·1574−11	−0·1316−11	−0·1966−11	−0·6820−12	0·1077−11
43	0·3552−11	−0·1217−11	−0·6288−12	−0·2158−11	−0·4505−12	−0·5591−12
44	0·1092−10	−0·4179−10	−0·2998−10	−0·2848−10	0·1839−10	0·2561−10
			(*e*) **F**[A]			
11	−0·8163−16	−0·5000−18	−0·1355−16	0·1401−16	0·9887−17	0·3099−16
21	0·4319−11	−0·5301−10	−0·6165−10	0·2049−10	0·1535−10	−0·5894−10
22	0·1685−15	0·2742−17	0·2500−17	−0·6686−16	−0·2075−16	0·8435−17
31	0·7120−11	0·8136−11	−0·1530−12	−0·6218−12	−0·1063−11	−0·9791−12
32	−0·9984−10	−0·7592−10	−0·6709−10	−0·2376−10	0·2293−10	−0·9547−10
33	0·4929−15	0·6011−17	0·2063−16	−0·1589−15	−0·5346−16	−0·1935−16
41	0·1151−10	−0·5387−10	−0·3453−10	0·2859−10	−0·3322−10	−0·2506−10
42	−0·2164−09	0·7402−09	0·5076−09	0·4978−09	0·4129−09	−0·3856−09
43	0·1842−10	−0·7437−10	−0·3819−10	−0·5401−10	−0·4561−10	−0·3084−10
44	−0·9081−16	0·7142−18	−0·7956−17	0·1440−16	0·3503−17	0·3076−16

[A] Note: $F(i,j) = -F(j,i)$.

Table 5. Ro–vibrational energy levels (in cm^{-1}) of the C_{2v} isotopes of H_2O^+

(a) $H_2{}^{16}O^+$

E_{vib}	0.000	1412.107	2780.651	3212.474	3254.973
J K_a K_c					
1 0 1	20.881	21.125	21.351	20.439	20.219
1 1 1	37.224	41.368	46.836	36.279	35.478
1 1 0	41.174	45.143	50.375	40.169	39.743
2 0 2	61.988	62.886	63.691	60.686	84.173
2 1 2	75.067	79.883	86.034	73.360	89.871
2 1 1	86.872	91.162	96.628	84.941	90.109
2 2 1	135.442	151.011	171.465	102.311	129.867
2 2 0	136.100	151.507	171.795	114.251	130.599
3 0 3	122.133	124.285	126.275	119.611	154.087
3 1 3	131.403	137.317	144.588	128.526	190.678
3 1 2	154.943	159.855	165.712	151.705	194.239
3 2 2	198.235	214.590	235.705	159.954	238.242
3 2 1	201.205	216.866	237.423	167.914	238.420
3 3 1	287.764	321.086	364.357	193.515	276.022
3 3 0	287.906	321.178	364.389	193.515	276.060
4 0 4	199.973	204.239	208.224	195.848	281.541
4 1 4	205.883	213.351	222.222	201.557	321.348
4 1 3	244.640	250.490	257.122	234.045	322.207
4 2 3	281.237	298.762	320.966	238.867	358.402
4 2 2	289.807	305.550	325.917	239.785	359.181
4 3 2	372.868	407.118	451.072	276.344	439.477
4 3 1	373.108	407.183	451.233	279.470	439.680
4 4 1	493.490	549.375	620.816	283.702	473.415
4 4 0	493.670	549.516	620.936	313.241	473.626
5 0 5	294.636	301.700	308.602	323.930	460.197
5 1 5	298.058	307.643	318.657	326.297	461.351
5 1 4	354.954	362.532	370.398	348.078	464.492
5 2 4	384.178	403.247	426.835	376.772	543.958
5 2 3	401.861	417.505	437.673	387.106	544.675
5 3 3	478.949	514.329	559.331	394.043	576.594
5 3 2	480.852	515.627	559.923	412.495	577.360
5 4 2	600.054	657.218	720.555	434.484	691.471
5 4 1	600.422	657.625	723.750	467.821	691.623
5 5 1	750.265	831.795	730.001	470.775	720.236
5 5 0	750.605	832.082	730.142	502.501	720.538

(b) $H_2{}^{18}O^+$

E_{vib}	0.000	1406.282	2769.416	3206.405	3241.781
J K_a K_c					
1 0 1	20.849	21.093	21.319	20.411	20.192
1 1 1	36.832	40.915	46.296	35.878	35.124
1 1 0	40.814	44.722	49.864	39.806	39.418
2 0 2	61.872	62.773	63.584	60.586	83.965
2 1 2	74.579	79.335	85.401	72.869	95.365
2 1 1	86.483	90.707	96.082	84.559	95.814

Table 5. *(Continued)*

2 2 1	133.984	149.319	169.443	95.083	128.546
2 2 0	134.664	149.831	169.785	106.640	129.298
3 0 3	121.843	124.014	126.028	119.329	159.745
3 1 3	130.761	136.617	143.808	127.906	189.223
3 1 2	154.492	159.338	165.106	151.280	192.954
3 2 2	196.681	212.797	233.583	152.523	242.132
3 2 1	199.755	215.154	235.359	160.219	242.263
3 3 1	284.562	317.396	360.005	186.426	273.109
3 3 0	284.708	317.490	360.035	191.506	273.153
4 0 4	199.399	203.708	207.747	195.313	280.176
4 1 4	205.014	212.432	221.235	200.683	325.214
4 1 3	244.070	249.863	256.418	226.385	325.997
4 2 3	279.538	296.824	318.703	230.918	355.370
4 2 2	288.370	303.824	323.814	239.252	356.228
4 3 2	369.570	403.316	446.597	273.222	440.898
4 3 1	369.839	403.400	446.768	273.222	441.079
4 4 1	487.915	543.023	613.445	282.310	468.322
4 4 0	488.095	543.163	613.562	304.587	468.544
5 0 5	293.680	300.807	307.798	315.846	451.235
5 1 5	296.889	306.436	317.400	318.139	458.234
5 1 4	354.169	361.724	369.543	347.383	461.485
5 2 4	382.267	401.106	424.382	375.472	545.301
5 2 3	400.437	415.777	435.549	378.616	545.970
5 3 3	475.528	510.390	554.709	392.683	571.379
5 3 2	477.535	511.751	555.338	403.595	572.179
5 4 2	594.366	650.725	722.465	426.000	689.800
5 4 1	594.728	651.126	722.583	464.457	689.943
5 5 1	741.753	822.218	724.771	467.443	712.433
5 5 0	742.090	822.502	727.802	486.423	712.745

(c) $D_2{}^{16}O^+$

E_{vib}	0.000	1047.539	2071.881	2346.609	2424.351
J K_a K_c					
1 0 1	10.642	10.735	10.825	10.478	10.395
1 1 1	20.281	21.847	23.738	19.993	19.555
1 1 0	22.115	23.628	25.453	21.793	21.518
2 0 2	31.682	32.004	32.311	31.195	30.886
2 1 2	39.739	41.545	43.681	39.167	38.371
2 1 1	45.230	46.878	48.820	44.553	44.278
2 2 1	74.016	79.998	87.218	72.986	71.646
2 2 0	74.260	80.200	87.375	73.239	71.926
3 0 3	62.665	63.408	64.124	61.737	78.155
3 1 3	68.770	70.960	73.490	67.768	78.273
3 1 2	79.731	81.618	83.749	78.524	78.482
3 2 2	105.983	112.256	119.738	104.514	102.754
3 2 1	107.122	113.209	120.535	105.604	104.265
3 3 1	158.202	171.272	186.983	138.783	153.169
3 3 0	158.242	171.299	186.986	144.192	153.179
4 0 4	103.022	104.459	105.849	101.497	123.050
4 1 4	107.236	109.963	113.043	105.712	144.199
4 1 3	125.369	127.601	130.044	123.530	147.966
4 2 3	148.363	155.053	162.938	146.261	191.701
4 2 2	151.690	157.886	165.258	149.553	193.515

Table 5. *(Continued)*

4 3 2	201.327	214.748	230.741	177.748	193.515
4 3 1	201.408	214.791	230.811	181.342	195.551
4 4 1	272.893	295.373	322.198	198.700	264.253
4 4 0	272.940	295.408	322.224	198.727	264.288
5 0 5	152.295	154.676	157.031	179.112	203.789
5 1 5	154.957	158.404	162.217	198.269	245.382
5 1 4	181.781	184.584	187.501	205.302	246.862
5 2 4	201.042	208.276	216.662	216.346	246.862
5 2 3	208.145	214.391	221.796	216.409	247.753
5 3 3	255.208	269.053	285.456	225.314	317.186
5 3 2	255.787	269.495	285.721	227.267	317.249
5 4 2	326.845	349.800	377.092	251.774	334.596
5 4 1	326.941	349.903	377.101	252.398	334.726
5 5 1	417.348	451.116	424.868	256.031	404.326
5 5 0	417.435	451.186	427.476	273.304	404.388
			(d) $D_2{}^{18}O^+$		
E_{vib}	0.000	1043.174	2063.397	2344.983	2412.851
J K_a K_c					
1 0 1	10.686	10.780	10.871	10.523	10.439
1 1 1	20.015	21.556	23.417	19.715	19.311
1 1 0	21.893	23.379	25.171	21.560	21.316
2 0 2	31.797	32.123	32.436	31.311	31.000
2 1 2	39.518	41.302	43.412	38.932	38.171
2 1 1	45.140	46.760	48.668	44.456	44.208
2 2 1	72.999	78.881	85.979	71.922	70.713
2 2 0	73.262	79.098	86.147	72.198	71.012
3 0 3	62.846	63.605	64.341	61.915	78.264
3 1 3	68.608	70.781	73.290	67.588	85.765
3 1 2	79.826	81.685	83.785	78.620	85.990
3 2 2	105.099	111.272	118.634	103.587	101.919
3 2 1	106.324	112.297	119.487	104.764	103.567
3 3 1	155.908	168.761	184.213	129.052	151.057
3 3 0	155.950	168.791	184.215	134.181	151.068
4 0 4	103.235	104.711	106.145	101.705	128.719
4 1 4	107.135	109.855	112.927	105.586	143.564
4 1 3	125.683	127.894	130.312	123.849	147.518
4 2 3	147.641	154.235	162.005	145.498	193.616
4 2 2	151.200	157.262	164.483	149.035	194.517
4 3 2	199.238	212.439	228.169	168.047	196.208
4 3 1	199.337	212.494	228.247	171.383	197.362
4 4 1	268.820	290.943	317.344	191.225	260.490
4 4 0	268.867	290.978	317.370	196.546	260.530
5 0 5	152.504	154.949	157.380	179.664	203.748
5 1 5	154.912	158.367	162.190	197.685	246.562
5 1 4	182.318	185.118	188.029	202.066	249.023
5 2 4	200.501	207.646	215.928	202.123	249.023
5 2 3	208.058	214.156	221.393	205.219	250.785
5 3 3	253.378	266.997	283.134	215.588	313.611
5 3 2	254.025	267.488	283.431	217.354	313.717
5 4 2	323.034	345.622	372.483	246.657	337.885
5 4 1	323.128	345.723	372.494	249.926	337.979
5 5 1	411.030	444.284	431.919	250.541	398.466

Table 5. *(Continued)*

5 5 0	411.116	444.354	434.262	262.952	398.530
			(e) $T_2{}^{16}O^+$		
E_{vib}	0.000	888.734	1760.903	1968.571	2067.184
J K_a K_c					
1 0 1	7.238	7.292	7.344	7.144	7.097
1 1 1	14.714	15.645	16.732	14.583	14.249
1 1 0	15.864	16.771	17.826	15.708	15.477
2 0 2	21.588	21.768	21.940	21.309	21.139
2 1 2	28.043	29.108	30.330	27.754	27.212
2 1 1	31.490	32.480	33.610	31.124	30.903
2 2 1	53.846	57.434	61.617	53.385	52.300
2 2 0	53.972	57.542	61.706	53.510	52.445
3 0 3	42.813	43.212	43.600	42.280	41.833
3 1 3	47.957	49.232	50.667	47.429	46.573
3 1 2	54.841	55.971	57.219	54.159	53.915
3 2 2	75.581	79.336	83.671	74.857	73.583
3 2 1	76.175	79.852	84.122	75.426	74.326
3 3 1	115.538	123.430	132.612	114.650	112.228
3 3 0	115.556	123.443	132.613	114.656	112.234
4 0 4	70.591	71.347	72.082	69.723	84.554
4 1 4	74.382	75.946	77.675	73.558	99.751
4 1 3	85.797	87.122	88.548	84.733	99.861
4 2 3	104.439	108.427	112.988	103.352	101.872
4 2 2	106.197	109.972	114.310	105.063	103.911
4 3 2	144.780	152.880	162.234	143.559	140.869
4 3 1	144.812	152.899	162.268	143.578	141.007
4 4 1	199.901	213.589	229.434	167.434	194.207
4 4 0	199.923	213.606	229.446	170.895	194.220
5 0 5	104.633	105.879	107.108	122.611	136.042
5 1 5	107.215	109.164	111.283	138.870	137.093
5 1 4	124.176	125.801	127.487	142.606	141.541
5 2 4	140.361	144.648	149.485	143.528	176.824
5 2 3	144.195	148.042	152.443	143.550	177.094
5 3 3	181.338	189.688	199.283	179.769	206.013
5 3 2	181.589	189.892	199.415	179.900	206.019
5 4 2	236.473	250.438	266.552	200.431	230.031
5 4 1	236.519	250.487	266.556	202.699	230.128
5 5 1	306.533	327.297	311.078	221.120	297.923
5 5 0	306.573	327.330	313.678	234.335	297.947
			(f) $T_2{}^{18}O^+$		
E_{vib}	0.000	880.530	1744.851	1957.327	2045.018
J K_a K_c					
1 0 1	7.214	7.267	7.319	7.121	7.074
1 1 1	14.334	15.235	16.285	14.194	13.893
1 1 0	15.510	16.385	17.403	15.346	15.144
2 0 2	21.504	21.683	21.857	21.228	21.058
2 1 2	27.589	28.623	29.809	27.290	26.787
2 1 1	31.112	32.068	33.159	30.743	30.548

Table 5. *(Continued)*

2 2 1	52.406	55.873	59.912	51.909	50.948
2 2 0	52.544	55.991	60.009	52.046	51.105
3 0 3	42.613	43.016	43.411	42.087	41.634
3 1 3	47.385	48.630	50.031	46.848	46.038
3 1 2	54.420	55.514	56.721	53.744	53.519
3 2 2	74.067	77.699	81.889	73.310	72.162
3 2 1	74.715	78.261	82.378	73.934	72.962
3 3 1	112.339	119.968	128.837	111.369	109.222
3 3 0	112.358	119.982	128.838	111.372	109.230
4 0 4	70.200	70.969	71.722	69.341	84.037
4 1 4	73.642	75.179	76.878	72.810	100.351
4 1 3	85.302	86.591	87.979	84.253	102.540
4 2 3	102.818	106.681	111.098	101.703	104.916
4 2 2	104.722	108.354	112.529	103.566	105.000
4 3 2	141.500	149.331	158.368	140.205	137.784
4 3 1	141.541	149.357	158.407	140.225	137.939
4 4 1	194.268	207.509	222.830	156.126	188.903
4 4 0	194.289	207.526	222.841	159.266	188.916
5 0 5	103.967	105.238	106.499	122.022	140.175
5 1 5	106.254	108.179	110.275	128.587	140.912
5 1 4	123.558	125.153	126.808	128.609	141.073
5 2 4	138.591	142.754	147.450	137.079	173.652
5 2 3	142.723	146.413	150.639	141.124	173.954
5 3 3	177.958	186.032	195.307	176.349	207.950
5 3 2	178.245	186.263	195.459	176.479	207.970
5 4 2	230.738	244.248	259.830	188.823	224.613
5 4 1	230.782	244.295	259.834	190.868	224.722
5 5 1	297.818	317.925	315.229	209.449	289.700
5 5 0	297.858	317.957	317.517	223.110	289.725

calculated rotational levels for the first five low-lying vibrational states up to $J = 5$ using ten vibrational basis functions. In order to ensure convergence of the calculated eigenenergies with respect to the basis set used, a number of truncated basis sets were investigated. Calculations were employed using five vibrational basis functions up to the same J level. It was found that the mean difference of the rotational levels of the first five vibrational states using five and ten vibrational basis sets was $4{\cdot}6\ \mathrm{cm}^{-1}$ for all J.

4. Discussion

The theoretical ro–vibrational states for the ground electronic state χ^2B_1 of H_2O^+ have been calculated using the discrete potential of Weis *et al.* (1989). The ro–vibrational Hamiltonian takes into full account mechanical anharmonicity, as well as ro–vibrational coupling effects. However, nuclear spin interactions, the electron spin–rotation interaction and the electronic angular momentum–rotation interaction (commonly referred to as the Renner–Teller effect) have been neglected in the calculations. Although the χ^2B_1 and A^2A_1 of H_2O^+ ion form a Renner–Teller pair, it is appropriate to treat the electronic ground state PE function as a single state problem near the PE minimum. Renner–Teller coupling effects need to be included in regions of the potential closed to the linear structures.

The $P(3,6)$ analytical representation, given in Table 1, accurately mimics experimental structures near equilibrium geometry. The experimental equilibrium O–H bond length and H–O–H bond angle, given by Dinelli *et al.* (1988), are 1·001 Å and 108·9° respectively, which are in excellent agreement with the $P(3,6)$ fitted result of 1·0004 Å and 109·07° respectively. Both are in excellent agreement with the fitted result of Weis *et al.* (1989), who obtained values of 1·0004 Å and 109·06° respectively. Furthermore, both the theoretically calculated r_0 and α_0 structures agree to within 0·002 Å and 0·2° with the experimental structures of Lew (1976) and Dinelli *et al.* (1988).

Table 2 gives the zero-point energies and assignments of the 20 lowest-lying vibrational band origins. Care must be taken with the ZPE since the centre of global expansion may be below the PE minimum. Nevertheless, from the errors associated with the fit, the ZPE are expected to be accurate to within $\pm 6\ \mathrm{cm}^{-1}$.

The assignments in Table 2 are determined from the weights of the coefficients via

$$\%\mathrm{Weight} = \{C_{ij}^2 / \sum C_{ij}^2\}^{1/2} \times 100\,, \tag{7}$$

where the C are the coefficients of the vibrational basis functions. The assignments of the 20 lowest-lying vibrational band origins yielded by the t coordinate calculations are identical for all C_{2v} isotopes of H_2O^+.

Table 3 compares the lowest 20 experimental vibrational band origins of H_2O^+ and D_2O^+ (where available) with ab initio calculated variational and perturbation theories. The perturbation theory employed by Weis *et al.* (1989) included the Darling–Dennison corrections. All calculations are in essentially good agreement with the available experimental data even though the variational approach employed here is vastly different in form and substance from that used by Weis *et al.* (1989). For H_2O^+ the maximum difference between the experimetal data and the t coordinate and internal coordinate solutions is 44 and 135 cm^{-1} respectively. Similarly for D_2O^+ the maximum errors are 25 and 19 cm^{-1} respectively. Although agreement between the t coordinate and internal coordinate variational solutions is particularly good for D_2O^+, the major discrepancy between these as well as the perturbation calculations for both H_2O^+ and D_2O^+ arises from states highly excited in the bending mode. The bend potential is shallow and so states that are highly excited in the bending mode are extremely sensitive to basis set incompleteness. With respect to our solution algorithm one would need to incorporate a total list far greater than 560 basis functions and, in particular, a configuration list incorporating more t_2 functions. However, as will be shown below, the t coordinate approach reproduces ro–vibrational transition energies to high accuracy when compared with experiment for the ground and first excited vibrational states. For these vibrational states both variational calculations are in excellent agreement and so have converged with respect to the basis set expansions.

Both variational calculations give the same assignment for H_2O^+, differing only in the order of the last three vibrational band origins for D_2O^+. The t coordinate result for H_2O^+ and D_2O^+ yields the sequence (060) < (210) < (111), which

Table 6. Comparison of experimental with calculated low-lying ro–vibrational states of $H_2{}^{16}O^+$ and $D_2{}^{16}O^+$ (in cm^{-1})

(a) $H_2{}^{16}O^+$

J	K_a	K_c	This Work	Expt.[a]	Δ	This Work	Expt.[a]	Δ
			(000)[b]			(010)[b]		
1	0	1	20.88	20.86	0.02	21.13	20.76	0.37
1	1	1	37.22	37.19	0.03	41.37	41.20	0.17
1	1	0	41.17	41.10	0.07	45.14	45.30	-0.16
2	0	2	61.99	61.96	0.03	62.89	61.73	1.16
2	1	2	75.07	75.09	-0.02	79.88	78.78	1.10
2	1	1	86.87	86.85	0.02	91.16	91.10	0.06
2	2	1	135.44	135.67	-0.23	151.01	151.97	-0.96
2	2	0	136.10	136.29	-0.19	151.51	152.52	-1.01
3	0	3	122.13	122.12	0.01	124.29	121.81	2.48
3	1	3	131.40	131.48	-0.08	137.32	134.63	2.69
3	1	2	154.94	154.89	0.05	159.86	159.23	0.63
3	2	2	198.24	198.47	-0.23	214.59	214.63	-0.04
3	2	1	201.21	201.48	-0.27	216.87	217.32	-0.45
3	3	1	287.76	288.76	-1.00	321.09	324.01	-2.92
3	3	0	287.91	288.82	-0.90	321.18	324.05	-2.87
4	0	4	199.97	200.03	-0.06	204.24	199.68	4.54
4	1	4	205.88	205.98	-0.10	213.35	208.42	4.93
4	1	3	244.64	244.59	0.05	250.49	249.12	1.37
4	2	3	281.24	281.53	-0.29	298.76	297.49	1.27
4	2	2	289.81	289.90	-0.09	305.55	305.09	0.46
4	3	2	372.87	373.66	-0.79	407.12	408.65	-1.53
4	3	1	373.11	374.09	-0.98	407.18	408.98	-1.80
4	4	1	493.49	495.62	-2.13	549.38	554.39	-5.01
4	4	0	493.67	495.63	-1.96	549.52	554.39	-4.87
5	0	5	294.64	294.76	-0.12	301.70	294.27	7.43
5	1	5	298.06	298.22	-0.16	307.64	299.74	7.90
5	1	4	354.95	354.94	0.01	362.53	359.88	2.65
5	2	4	384.18	384.37	-0.19	403.25	399.93	3.32
5	2	3	401.86	401.89	-0.03	417.51	416.37	1.14
5	3	3	478.95	479.66	-0.71	514.33	514.29	0.04
5	3	2	480.85	481.31	-0.46	515.63	515.56	0.07
5	4	2	600.05	601.90	-1.85	657.22	660.42	-3.20
5	4	1	600.42	601.94	-1.52	657.63	660.45	-2.82
5	5	1	750.27	753.37	-3.11	831.80	837.02	-5.22
5	5	0	750.61	753.38	-2.77	832.08	837.02	-4.94

is consistent with the internal coordinate result for H_2O^+, but in the case of D_2O^+ the sequence is (210) < (111) < (012). The t coordinate assignment appears more consistent with the experimental results. For example, for H_2O^+ and D_2O^+ the seventeenth band origin has experimental values of 7639 and 5650 cm^{-1}, respectively, compared with the t coordinate result of 7631 and 5675 cm^{-1}. The internal coordinate result of Weis *et al.* (1989) gives values of 7662 and 5666 cm^{-1} respectively. Furthermore, for H_2O^+ Weis *et al.* gave the (060) band origin at

Table 6. *(Continued)*

(b) $D_2{}^{16}O^+$

J K_a K_c	This Work	Expt.[c]	Δ	This Work	Expt.[c]	Δ
		(000)[b]			(010)[b]	
1 0 1	10.64	10.62	0.02	10.74	10.60	0.14
1 1 1	20.28	20.28	0.00	21.85	21.83	0.02
1 1 0	22.12	22.10	0.02	23.63	23.73	-0.10
2 0 2	31.68	31.65	0.03	32.00	31.59	0.41
2 1 2	39.74	39.78	-0.04	41.55	41.21	0.34
2 1 1	45.23	45.23	0.00	46.88	46.90	-0.02
2 2 1	74.02	74.25	-0.23	80.00	80.59	-0.59
2 2 0	74.26	74.48	-0.22	80.20	80.81	-0.61
3 0 3	62.67	62.65	0.02	63.41	62.53	0.88
3 1 3	68.77	68.84	-0.07	70.96	70.08	0.88
3 1 2	79.73	79.72	0.01	81.62	81.44	0.16
3 2 2	105.98	106.27	-0.29	112.26	112.55	-0.29
3 2 1	107.12	107.39	-0.27	113.21	113.63	-0.42
3 3 1	158.20	159.05	-0.85	171.27	173.00	-1.73
3 3 0	158.24	159.06	-0.82	171.30	173.02	-1.72
4 0 4	103.02	103.04	-0.02	104.46	102.88	1.58
4 1 4	107.24	107.33	-0.09	109.96	108.30	1.66
4 1 3	125.37	125.35	0.02	127.60	127.16	0.44
4 2 3	148.36	148.68	-0.32	155.05	154.99	0.06
4 2 2	151.69	151.91	-0.22	157.89	157.98	-0.10
4 3 2	201.33	202.16	-0.83	214.75	216.04	-1.29
4 3 1	201.41	202.29	-0.88	214.79	216.15	-1.36
4 4 1	272.89	274.55	-1.66	295.37	298.64	-3.27
4 4 0	272.94	274.55	-1.61	295.41	298.64	-3.23
5 0 5	152.30	152.37	-0.07	154.68	152.11	2.57
5 1 5	154.96	155.09	-0.13	158.40	155.70	2.70
5 1 4	181.78	181.79	-0.01	184.58	183.72	0.88
5 2 4	201.04	201.36	-0.32	208.28	207.41	0.87
5 2 3	208.15	208.32	-0.17	214.39	214.20	0.19
5 3 3	255.21	256.05	-0.84	269.05	269.80	-0.75
5 3 2	255.79	256.55	-0.76	269.50	270.24	-0.74
5 4 2	326.85	328.48	-1.63	349.80	352.47	-2.67
5 4 1	326.94	328.49	-1.55	349.90	352.48	-2.58
5 5 1	417.35	419.24	-1.89	451.12	455.78	-4.66
5 5 0	417.43	419.24	-1.81	451.19	455.78	-4.61

a) See Lew (1976).

b) Vibrational state.

c) See Lew and Groleau (1987).

$7496 \cdot 6\ cm^{-1}$. Nevertheless, care must be taken to avoid over-interpreting these results for these high lying vibrational band origins, because of basis set incompleteness.

Table 4 gives the vibrationally averaged rotational constants spanned over the four low-lying vibrational wavefunctions. From least squares fits to the diagonal elements

of the H_2O^+ rotational constants spanned by the lowest 20 vibrational wavefunctions, the spectroscopic constants $(A_e, A_o, B_e, B_o, C_e, C_o)$ using the t coordinate solution are $(28{\cdot}82, 28{\cdot}79, 12{\cdot}59, 12{\cdot}41, 8{\cdot}69, 8{\cdot}46)$ cm^{-1} respectively. This compares favourably with experimental values of $(27{\cdot}79, 29{\cdot}04, 12{\cdot}60, 12{\cdot}42, 8{\cdot}71, 8{\cdot}47)$ cm^{-1} respectively, given by Dinelli *et al.* (1988), and with the calculated values of $(27{\cdot}96, 28{\cdot}77, 12{\cdot}60, 12{\cdot}42, 8{\cdot}68, 8{\cdot}45)$ cm^{-1} given by Weis *et al.* (1989).

The limiting case for the rotational levels of all $C_{2\nu}$ isotopes of H_2O^+ is Mulliken's prolate symmetric top. This is reflected by the Ray asymmetry parameter which for $H_2{}^{16}O^+$, $D_2{}^{16}O^+$, $T_2{}^{16}O^+$, $H_2{}^{18}O^+$, $D_2{}^{18}O^+$ and $T_2{}^{18}O^+$ has been calculated using the t coordinate solution to be $-0{\cdot}612, -0{\cdot}680, -0{\cdot}733, -0{\cdot}602, -0{\cdot}665$ and $-0{\cdot}716$ respectively. Hence, the rotational levels can be assigned within this framework. Table 5 give the rotational energy levels for the first five vibrational states for all the $C_{2\nu}$ isotopes of H_2O^+. Experimental data for any of the $C_{2\nu}$ isotopes are scarce, with H_2O^+ and D_2O^+ being exceptions. Table 6 compares the experimentally observed rotational levels of the ground and first excited vibrational states of H_2O^+ and D_2O^+ with those calculated using our t coordinate solution algorithm. The agreement between experiment and theory is excellent, with a maximum deviation of 8 cm^{-1} occuring for the $J = 5$, $K_a = 1$ and $K_c = 5$ state of the first excited vibrational level of H_2O^+. Smaller deviations occur for all the other states. For example, on comparison with experiment the calculated rotational levels of the ground and first excited vibrational states of D_2O^+ agree to within 2 and 5 cm^{-1} respectively. Errors of a similar magnitude were also encountered in the internal coordinate solution by Weis *et al.* Hence, our calculations confirm the experimental assignment and so provide further evidence that both the t coordinate and internal coordinate solution algorithms have converged for the rotational levels of the ground and first excited vibrational states of H_2O^+ and D_2O^+. Therefore, confidence can be placed in the assignments and in the calculated eigenenergies of the rotational levels for all of the other $C_{2\nu}$ isotopes of H_2O^+ given in Table 5.

5. Conclusions

A t coordinate ro–vibrational Hamiltonian has been used in order to theoretically calculate the rotationally resolved infrared spectrum of all the $C_{2\nu}$ isotopes of H_2O^+ in its ground electronic state (χ^2B_1). The solution algorithm utilised a Padé approximate analytical representation of the discrete potential energy surface of Weis *et al.* (1989) and a finite-element method in order to construct three-dimensional basis functions. The variational solution yielded ro–vibrational wavefunctions and eigenvalues which are in excellent agreement with experiment for the rotational levels of the ground and first excited vibrational states of H_2O^+ and D_2O^+. Moreover, where comparisons could be made the t coordinate solution algorithm was in excellent agreement with that used by Weis *et al.*, who employed an internal coordinate ro–vibrational Hamiltonian and a combination of Morse, harmonic oscillator and associate Legendre functions for their trial basis functions. Ab initio calculated rotationally resolved data are presented for isotopes of H_2O^+ for which there are no experimental data.

Acknowledgments

All calculations were performed on a VAX 8850 and VAX 3100 work station; the former was made available through the generous support of the Computing Centre of the University of Newcastle. We would like to acknowledge the support of the Research Management Committee, University of Newcastle. We wish to acknowledge the Overseas Postgraduate Research Award held by F. Wang.

References

Burton, P. G., von Nagy-Felsobuki, E. I., Doherty, G., and Hamilton, M. (1985). *Mol. Phys.* **55**, 527.
Carney, G. D., Langoff, S. R., and Curtiss, L. A. (1977). *J. Chem. Phys.* **66**, 3724.
Carney, G. D., and Porter, R. N. (1976). *J. Chem. Phys.* **65**, 3547.
Carney, G. D., and Porter, R. N. (1980). *Phys. Rev. Lett.* **45**, 537.
Dinelli, B. M., Crofton, M. W., and Oka, T. (1988). *J. Mol. Spectrosc.* **127**, 1.
Doherty, G., Hamilton, M., Burton, P. G., and von Nagy-Felsobuki, E. I. (1986). *Aust. J. Phys.* **39**, 749.
Harris, D. O., Engerholm, G. G., and Gwinn, W. D. (1965). *J. Chem. Phys.* **43**, 1515.
Henderson, J. R., Miller, S., and Tennyson, J. (1988). *Spectrochim. Acta* A **44**, 1287.
Herzberg, G. (1980). *Ann. Geol.* **36**, 605.
Karlsson, L., Mattson, L., Jardrny, R., Albridge, R. G., Pinchas, S., Bergmark, T., and Siegbahn, K. (1975). *J. Chem. Phys.* **62**, 4745.
Lew, H. (1976). *Can. J. Phys.* **54**, 2028.
Lew, H., and Groleau, R. (1987). *Can. J. Phys.* **65**, 739.
Miller, S., Tennyson, J., and Sutcliffe, B. T. (1989). *Mol. Phys.* **66**, 429.
Ogilvie, J. F. (1981). *Proc. R. Soc. London* A **378**, 287.
Reutt, J. E., Wang, L. S., Lee, Y. T., and Shirley, D. A. (1986). *J. Chem. Phys.* **85**, 6928.
Searles, D. J., Dunne, S. J., and von Nagy-Felsobuki, E. I. (1988). *Spectrochim. Acta* A **44**, 505.
Searles, D. J., and von Nagy-Felsobuki, E. I. (1989). *Aust. J. Chem.* **42**, 737.
Searles, D. J., and von Nagy-Felsobuki, E. I. (1991*a*). *In* 'Vibrational Spectra and Structure', Vol. 19 (Ed. D. R. Durig), Chapt. 4 (Elsevier: Amsterdam).
Searles, D. J., and von Nagy-Felsobuki, E. I. (1991*b*). *J. Chem. Phys.* **95**, 1107.
Searles, D. J., and von Nagy-Felsobuki, E. I. (1991*c*). *Phys. Rev.* A **43**, 3365.
Strahan, S. E., Mueller, R. P., and Saykally, R. J. (1986). *J. Chem. Phys.* **85**, 1252.
Sutcliffe, B. T. (1990). *In* 'Methods of Computational Chemistry', Vol. 5 (Ed. S. Wilson) (Plenum: New York).
Tennyson, J., and Sutcliffe, B. T. (1984). *Mol. Phys.* **51**, 887.
Watson, J. K. (1968). *Mol. Phys.* **15**, 479.
Watson, J. K. (1970). *Mol. Phys.* **19**, 465.
Weis, B., Carter, S., Rosmus, P., Werner, H.-J., and Knowles, P. J. (1989). *J. Chem. Phys.* **91**, 2818.

Manuscript received 28 January, accepted 15 May 1992